

Final Draft
of the original manuscript:

Trojanova, Z.; Lukac, P.; Kainer, K.U.:
**Stress Relaxation in AX41 Magnesium Alloy Studied at Elevated
Temperatures**
In: Advanced Engineering Materials (2007) Wiley

DOI: 10.1002/adem.200700018

Stress relaxation in AX41 magnesium alloy studied at elevated temperatures.

By Zuzanka Trojanová*, Pavel Lukáč, Karl Ulrich Kainer

Magnesium alloy AX41 has been deformed at elevated temperatures. Stress relaxation tests were performed in order to reveal features of the thermally activated dislocation motion. Internal and effective components of the applied stress have been estimated. Apparent activation volume decreases with the increasing effective stress. Estimated values of the activation volume as well as the activation enthalpy indicate that the main thermally activated process is connected with the rapid decrease of the internal stress.

1. Introduction

For recent years, research and development of magnesium alloys have shown that the Mg-based alloys have great potential for applications as the lightweight materials. Among them, the Mg-Al-Ca alloys exhibit good resistance due to the presence of a heat-stable phase. During plastic deformation in a certain range of temperature and strain rate, different micromechanisms may play an important role. The analysis of deformation microstructures has shown that one should consider dislocation-based mechanisms in order to explain the deformation behaviour. It is widely accepted that the resolved shear stress τ necessary for the dislocation motion in the slip plane can be divided into two components:

$$\tau = \tau_i + \tau^*, \quad (1)$$

where τ_i is the (internal) athermal contribution to the stress, resulting from long-range internal stresses impeding the plastic flow.

$$\tau_i = \alpha_1 G b \rho_t^{1/2}, \quad (2)$$

* Prof. RNDr. Z. Trojanová, Prof. RNDr. P. Lukáč
Department of Metal Physics, Faculty Mathematics and Physics, Charles University, Prague
Ke Karlovu 5, CZ-121 16 Praha 2 (Czech Republic)
E-mail: ztrojan@met.mff.cuni.cz

where G is the shear modulus, α_1 is a constant describing interaction between dislocations, b is the Burgers vector of dislocations and ρ_t is the total dislocation density. The effective shear stress τ^* acts on dislocations during their thermally activated motion when they overcome short range obstacles. The mean velocity of dislocations v is connected with the plastic shear strain rate by the Orowan equation:

$$\dot{\gamma} = \rho_m b v \quad (3)$$

where ρ_m is the density of mobile dislocations. The dislocation velocity (the plastic shear strain rate) is controlled by obstacles (their strength, density) and it depends on temperature and the effective shear stress. In polycrystalline materials, the resolved shear stress τ and its components are related to the applied stress σ and its corresponding components by the Taylor orientation factor ψ : $\sigma = \psi\tau$. A simple relation between the resolved shear strain rate and strain rate is $\dot{\gamma} = \psi\dot{\epsilon}$.

The most common equation used in describing the average dislocation velocity as a function of the effective stress is an Arrhenius type. The plastic strain rate $\dot{\epsilon}$ for a single thermally activated process can be expressed as:

$$\dot{\epsilon} = \dot{\epsilon}_0 \exp\left[-\frac{\Delta G(\sigma^*)}{kT}\right], \quad (4)$$

where $\dot{\epsilon}_0$ is a pre-exponential factor containing the mobile dislocation density, the average area covered by the dislocations in every activation act, the dislocation Burgers vector, the vibration frequency of the dislocation line, and the geometric factor. T is the absolute temperature and k is the Boltzmann constant. $\Delta G(\sigma^*)$ is the change in the Gibbs free enthalpy depending on the effective stress $\sigma^* = \sigma_{ap} - \sigma_i$ and its simple form is

$$\Delta G(\sigma^*) = \Delta G_0 - V\sigma^* = \Delta G_0 - V(\sigma - \sigma_i). \quad (5)$$

Here ΔG_0 is the Gibbs free enthalpy necessary for overcoming a short range obstacle without the stress and $V = bdL$ is the activation volume where d is the obstacle wide and L is the mean length of dislocation segments between obstacles. It should be mentioned that L may depend on the stress acting on dislocation segments.

The stress relaxation (SR) technique has been demonstrated to be quite useful experimental method for estimating the activation volume and hence for determining the thermally activated process(es). In a stress relaxation test, the specimen is deformed to a certain stress σ_0 and then the machine is stopped and the stress is allowed to relax. The stress decreases with the time t . The specimen can be again reloaded and deformed to a higher stress and the stress relaxation test may be repeated. The time derivative $\dot{\sigma} = d\sigma/dt$ is the stress relaxation rate and $\sigma = \sigma(t)$ is the flow stress at time t during the SR. Stress relaxation tests are very often analysed under the assumption that the stress relaxation rate is proportional to the strain rate $\dot{\epsilon}$ according to [1] as:

$$\dot{\epsilon} = -\dot{\sigma}/M \quad (6)$$

where M is the combined modulus of the specimen – machine set.

Combining (3), (4), (5) and (6), we have

$$-\dot{\sigma} = M\dot{\epsilon}_0 \exp\left[-\frac{\Delta G_0 - V\sigma^*}{kT}\right]. \quad (7)$$

Taking the logarithm of this equation we get

$$\ln(-\dot{\sigma}) = \ln(M\dot{\epsilon}_0) - \frac{\Delta G_0}{kT} + \frac{V\sigma^*}{kT}. \quad (8)$$

The stress decrease with the time during the SR can be described by the well known Feltham equation [2]:

$$\Delta\sigma(t) = \sigma(0) - \sigma(t) = \alpha \ln(\beta t + 1), \quad (9)$$

where $\sigma(0) \equiv \sigma_0$ is the stress at the beginning of the stress relaxation at time $t = 0$,

$$\alpha = \frac{kT}{V}, \quad (10)$$

$$\beta = \frac{M\dot{\epsilon}_0 V}{kT} \exp\left[-\frac{\Delta G_0 - V\sigma^*(0)}{kT}\right] = \frac{M\dot{\epsilon}(0)}{\alpha}, \quad (11)$$

where $\dot{\epsilon}(0)$ the plastic strain rate at the beginning of the relaxation.

Most of die cast or squeeze cast magnesium alloys are Mg-Al alloys. Third alloying elements are used to improve properties of these alloys. Among the alloying elements Ca is a promising elemental addition as a cheaper and lighter alternative to rare earth elements, also contributes to high temperature properties. Thus, the Mg-Al-Ca systems are very important for further development.

The objective of this paper is to examine stress relaxation during plastic deformation of magnesium alloy AX41 at different temperatures. We shall use the stress relaxation tests to obtain the values of the activation volume and the activation volume stress dependence in order to identify thermally activated processes in magnesium alloy AX41.

2. Experimental procedure

Magnesium alloy AX41 (nominal composition 4 wt% Al, 1 wt% Ca, balance Mg) was prepared by the squeeze cast technology. Samples for tensile tests had a cylindrical form with a diameter of 5 mm and a gauge length of 25 mm. Samples were deformed in an INSTRON 5882 machine at a constant cross head speed giving an initial strain rate of $6.7 \times 10^{-5} \text{ s}^{-1}$ over the temperature range of 23 to 300 °C. Sequential stress relaxation tests were performed at increasing stress along a stress-strain curve. Duration of the SR was 300 s. Ductility of the alloy at room temperature is very low and therefore only one SR test could be performed at room temperature. On the other hand, recovery during the SR test was observed at 300 °C. Results obtained at this temperature were not taken into account because the above given equation describing the SR were derived under an assumption that the internal stress σ_i is constant during the SR. Only in the first SR test at this temperature, recovery may be considered to be negligible, i.e. σ_i is constant.

Components of the applied stress (σ_i , σ^*) were estimated using Li's method [3,4]. The SR curves were fitted to the power law function in the form: $\sigma - \sigma_i = [a(m-1)]^{\frac{1}{1-m}} (t + t_0)^{\frac{1}{1-m}}$, where a , t_0 and m are fitting parameters.

3. Results and discussion

A part of the true stress-true strain curve at 100 °C with indicating the stresses at which the SR tests were performed is shown in Figure 1. Blank circles and full squares depict the stress at the end of the SR test σ_R and the internal stress σ_i , respectively. It is obvious that the internal stress σ_i form the substantial contribution to the applied stress σ_{ap} . Similar dependences obtained at 200 °C are given in Figure 2. It can be seen that the true stress-true strain curve obtained at 200 °C is more flat than that measured at 100 °C. The work hardening at 200 °C is lower. On the other hand, the SR was more pronounced, i.e. the stress decrease during the SR at 200 °C is higher than at 100 °C. It is also obvious that the internal stress component of the applied stress decreases with increasing strain. Figure 3 shows the variation of the effective (thermal stress) $\sigma^* = \sigma_i - \sigma_{ap}$ with strain for three deformation temperatures. It can be seen that the values of thermal stresses at a given strain are practically the same, independent of the testing temperature.

The dislocation (true) activation volume V_d is done by the following equation

$$V_d = \left(\frac{\partial \Delta G}{\partial \tau^*} \right)_{T,s} = kT \left(\frac{\partial \ln(\dot{\gamma}/\dot{\gamma}_0)}{\partial \tau^*} \right)_{T,s}, \quad (12)$$

where the subscripts T and s indicate that both the temperature and the dislocation microstructure (especially the mobile dislocation density) must be constant during the test. Equation (12) is usually used for the activation volume estimation in tests with changes in shear strain rate (or strain rate). $\dot{\epsilon}_0$ term is essentially structure-dependent and can be expressed as

$$\dot{\epsilon}_0 = (1/\psi) \rho_m b \frac{A}{\ell_c} v_D \frac{b}{\ell_c}. \quad (13)$$

where A is the mean area swept by the dislocation segment per successful thermally activated event, v_D is the Debye frequency and ℓ_c is the critical dislocation length for the thermally activated process to occur. In the stress relaxation experiments of polycrystals, it is only possible to record the variation of the applied stress σ_{ap} associated with the change in plastic strain rate (stress relaxation rate) and to determine an apparent activation volume, V_{app} , by using the expression

$$V_{app} = kT \left(\frac{d \ln(-\dot{\sigma})}{d \sigma_{ap}} \right)_T = \frac{kT}{\alpha} \quad (14)$$

A comparison of relations (5), (12) and (14) indicates that, at a given temperature, V_d and V_{app} are related by

$$V_{app} = \left((1/\psi)V_d + \frac{\partial \ln \dot{\epsilon}_0}{\partial \sigma^*} \right) \left(\frac{\partial \sigma^*}{\partial \sigma_{ap}} \right). \quad (15)$$

Considering the mobile dislocation density and the internal stress are constant, the relationship (14) can be written as $V_{app}=(1/\psi)V_d$.

Apparent activation volumes V_{app} for AX41 magnesium alloy polycrystals were estimated using equations (9) and (10). As usual, the values of V divided by b^3 are plotted against the applied stress. It is done for three testing temperatures in Figure 4. It can be seen that the apparent activation volumes decrease with applied stress for all temperatures measured. If the activation volumes for all temperatures are plotted against the thermal stress σ^* , the values appear to lie on one line - “master curve” (Figure 5). Similar curve has been estimated for the strain dependence of the activation volume (Figure 6). Kocks et al. [5] suggested an empirical equation between the Gibbs enthalpy ΔG and the effective stress σ^* in the following form:

$$\Delta G = \Delta G_0 \left[1 - \left(\frac{\sigma^*}{\sigma_0^*} \right)^p \right]^q, \quad (16)$$

where ΔG_0 and σ_0^* are Gibbs enthalpy and the effective stress at 0 K. From (4) and (15) it follows:

$$\sigma^* = \sigma_0^* \left[1 - \left(\frac{kT}{\Delta G_0} \ln \frac{\dot{\epsilon}_0}{\dot{\epsilon}} \right)^{1/q} \right]^{1/p}, \quad (17)$$

where p and q are phenomenological parameters reflecting the shape of a resistance profile. The possible ranges of values p and q are limited by the conditions $0 < p \leq 1$ and $1 \leq q \leq 2$. Ono [6], suggested that Equation (16) with $p = 1/2$, $q = 3/2$ describes a barrier shape profile that fits many predicted barrier shapes. Equation (17) can be rewritten

$$\dot{\epsilon} = \dot{\epsilon}_0 \exp \left[- \frac{\Delta G_0}{kT} \left(1 - \left(\frac{\sigma^*}{\sigma_0^*} \right)^p \right)^q \right] \quad (18)$$

and for the activation volume one obtains:

$$V = kT \frac{\partial \ln \dot{\epsilon} / \dot{\epsilon}_0}{\partial \sigma^*} = \frac{\Delta G_0 p q}{\sigma_0^*} \left[1 - \left(\frac{\sigma^*}{\sigma_0^*} \right)^p \right]^{q-1} \left(\frac{\sigma^*}{\sigma_0^*} \right)^{p-1}. \quad (19)$$

The values of the activation volume should lie at the curve given by the equation (19). The experimental values were fitted using equation (19) for various values p and q . The best correlation with the experimental data has been found for $p = 1/2$, $q = 2$ and the activation enthalpy value $\Delta G_0 = 0.96$ eV. It can be seen from Figure 5 that the dependence (19) describes well the experimental results. Using binominal expansion in (19), the activation volume should depends on the effective stress $V_{app} \propto (\sigma^*)^{-n}$. Generally, the values of the power exponent found in the literature vary from -0.5 to -1 [5].

The activation enthalpy $\Delta H = \Delta G - T\Delta S$ (ΔS is the entropy) is done by

$$\Delta H = -TV_d \frac{\partial \tau^*}{\partial T}. \quad (20)$$

For polycrystals, we can measure experimentally $\partial \sigma / \partial T$. Substituting from (12) into (20) it follows for the activation enthalpy

$$\Delta H = -T \cdot V_{app} \left(\frac{\partial \sigma}{\partial \tau^*} \right) \left(\frac{\partial \sigma}{\partial T} \right) \left(\frac{\partial \tau^*}{\partial \sigma} \right) = -TV_{app} \left(\frac{\partial \sigma}{\partial T} \right). \quad (21)$$

The activation enthalpy calculated according to (21) for 100 °C gives (0.95 ± 0.05) eV. The same value of 0.95 eV has been estimated for Mg in creep experiments at 400 K [7,8]. The values of the activation volume and the activation enthalpy may help to identify thermally activated process. Consider some of the common short range barriers to dislocation motion [9]. The dislocation–dislocation interaction mechanism has an activation volume ranging from about 10^2 – 10^4 b^3 , with the activation volume and enthalpy varying with strain. A rapid decrease in the internal stress with temperature (see Figure 7) indicates that softening is connected with dynamic recovery.

The AX41 alloy, with hcp structure, may deform on many possible glide systems with dislocations of Burgers vector $\langle a \rangle = 1/3[11\bar{2}0]$ in basal, prismatic and first order pyramidal planes and with dislocations of Burgers vector $\langle c+a \rangle = 1/3[11\bar{2}3]$ in first and second order pyramidal planes. The main deformation mode in magnesium is basal slip of $\langle a \rangle$ dislocations. The secondary conservative slip may be realised by $\langle a \rangle$ dislocations on prismatic and

pyramidal of the first order. Couret and Caillard [10,11] studied by TEM prismatic glide in magnesium in a wide temperature interval. They showed that the screw dislocations with the Burgers vector of $1/3[11\bar{2}0]$ are able to glide on prismatic planes and their mobility is much lower than the mobility of edge dislocations. The deformation is controlled by thermally activated glide of those screw dislocation segments. A single controlling mechanism has been identified as the Friedel-Escaig cross slip mechanism. This mechanism assumes a dissociated dislocation on a compact plane (0001) that joints together along a critical length L_r producing double kinks on non-compact plane. The activation volume is proportional to the critical length between two kinks. Amadieh et al. [12] found for the activation volume of the Friedel-Escaig mechanism value of $70 b^3$. Prismatic slip has been also observed by Koike and Ohyama [13] in the deformed AZ61 sheets. The activation of the prismatic slip and subsequent annihilation of the dislocation segments with the opposite sign are probably the main reason for the observed internal stress decrease. The double cross slip may be thermally activated process controlling the dislocation velocity. Beside of this mechanism, the thermally activated glide of the $\langle c+a \rangle$ dislocations should be taken into account. The internal stress acting on the dislocation is determined by the details of the internal structure at that moment and it is independent of the applied stress. The stress that changes when the applied stress is changed is only the effective stress. The internal stresses during plastic deformation of this alloy can be considered as the sum of stresses resulting from various dislocation arrangements and obstacles existing in the deformed material [14,15]. A decrease in the yield stress with increasing temperature and strain is very probably a consequence of dislocation annihilation during the deformation.

Conclusions

The main results of the complex analysis of the stress relaxation curves are:

- the internal stress decreases with increasing deformation temperature;
- the values of the apparent activation volumes are in the order of tens b^3 ;
- the activation volume depends on the thermal stress so that all values lie at the master curve $V_{app} \propto (\sigma^*)^n$;
- the estimated activation energy indicates that the main thermally activated process is very probably the glide of dislocations in the non-compact planes.

Acknowledgements

This work is a part of the research plan MSM 1M2560471601 that is financed by the Ministry of Education, Youth and Sports of the Czech Republic.

References

- [1] V.I. Dotsenko: *Phys. Stat. Sol. (b)* **1979**, 93, 11.
- [2] P. Feltham: *Phys. Stat. Sol.* **1963**, 3, 1340.
- [3] J.C.M. Li : *Canad. J. Appl. Phys.* **1967**, 45, 493.
- [4] R. De Batist, A. Callens : *Phys. Stat. Sol. (a)* **1974**, 21, 591.
- [5] U.F. Kocks, A.S. Argon, M.F. Ashby: *Progress in Mater. Sci.* **1975**, 19, 1.
- [6] K. Ono: *J. Appl. Phys.* **1968**, 39, 1803.
- [7] K. Milička, J. Čadek, P. Ryš: *Acta metall.* **1970**, 18, 1071.
- [8] S.S. Vagarali, T.G. Langdon: *Acta metall.* **1981**, 29, 1969.
- [9] A.G. Evans, R.D. Rawlings: *Phys. Stat. Sol.* **1969**, 34, 9.
- [10] A. Couret, D. Caillard: *Acta metall.* **1985**, 33, 1447.
- [11] A. Couret, D. Caillard: *Acta metall.* **1985**, 33, 1455.
- [12] A. Amadieh, J. Mitchell, J.E. Dorn: *Trans. AIME* **1965**, 233, 1130.
- [13] J. Koike, R. Ohyama: *Acta Mater.* **2005**, 53, 1963.
- [14] Z. Trojanová, P. Lukáč, K. Milička, Z. Záráz: *Mater. Sci. Eng. A* **2004**, 387-389, 80.
- [15] K. Milička, F. Dobeš, Z. Trojanová: *Mater. Sci. Eng. A* in press

Figure Captions

Fig. 1. A part of the true stress-true strain curve at 100 °C. The points on the curve indicate the stresses at which the SR tests were performed.

Fig. 2. A part of the true stress-true strain curve at 200 °C. The points on the curve indicate the stresses at which the SR tests were performed

Fig. 3. The strain variation of the effective stress at three different testing temperature

Fig. 4. The plot of the activation volume in b^3 against the applied stress

Fig. 5. The plot of the activation volume in b^3 against the thermal stress

Fig. 6. Strain dependence of the activation volume in b^3

Fig. 7. Variation of the internal stress with temperature

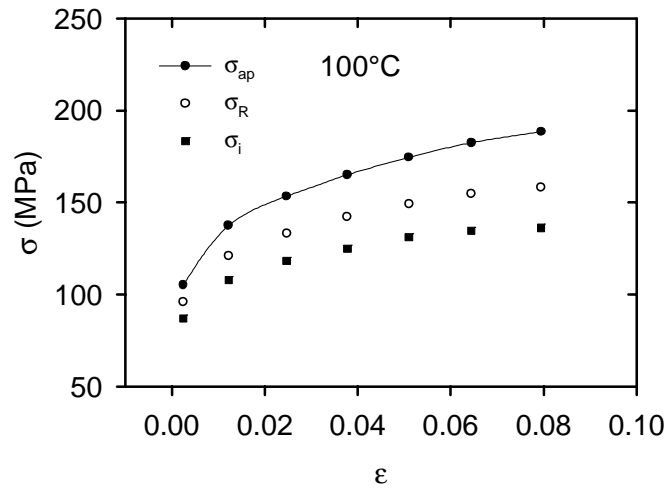


Fig. 1

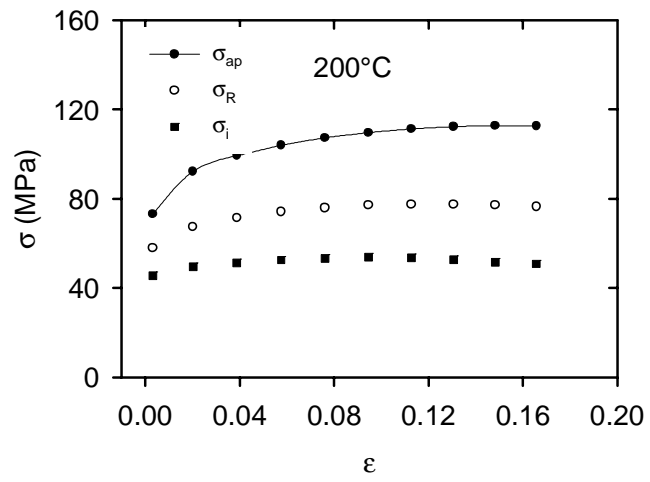


Fig. 2

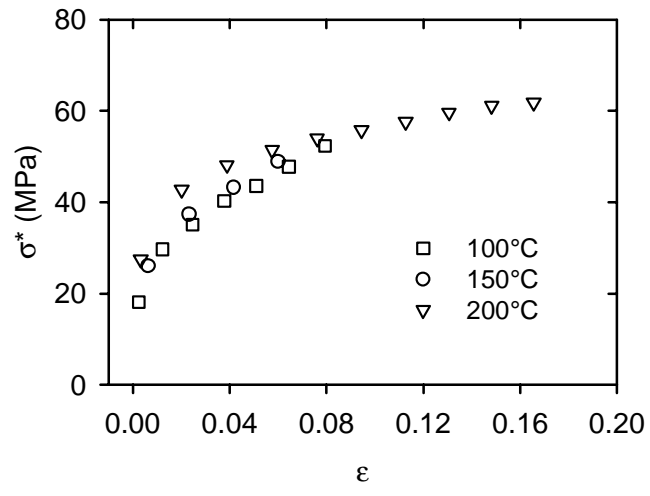


Fig. 3

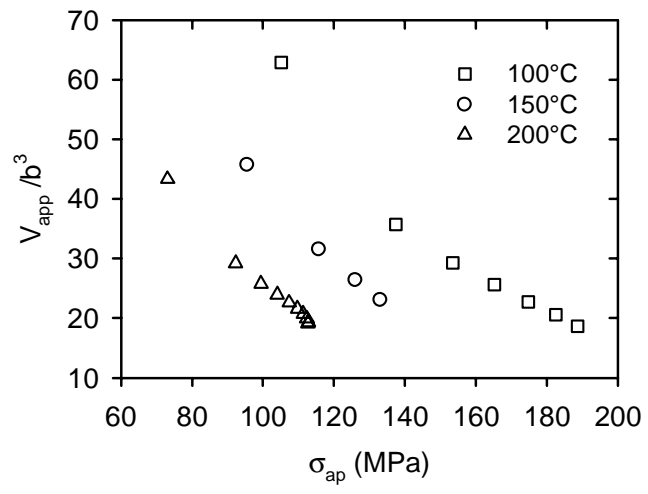


Fig. 4

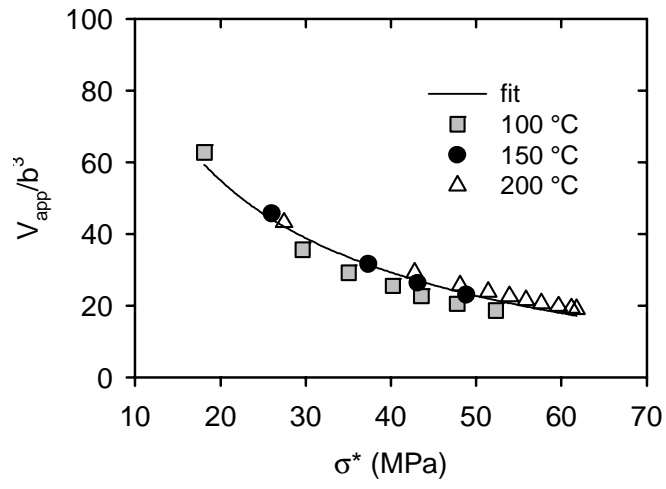


Fig. 5

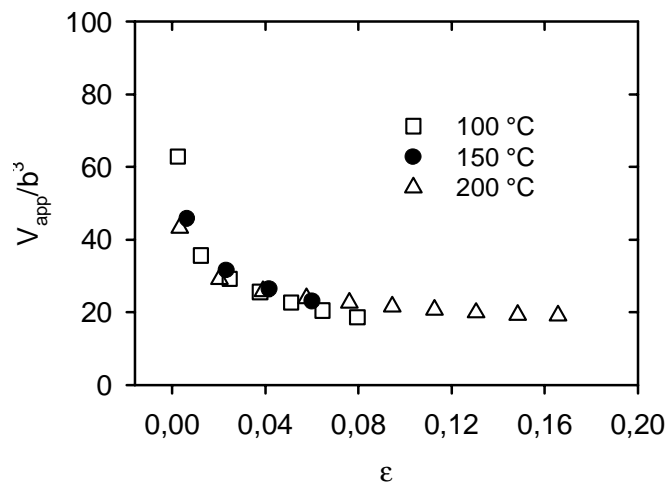


Fig. 6

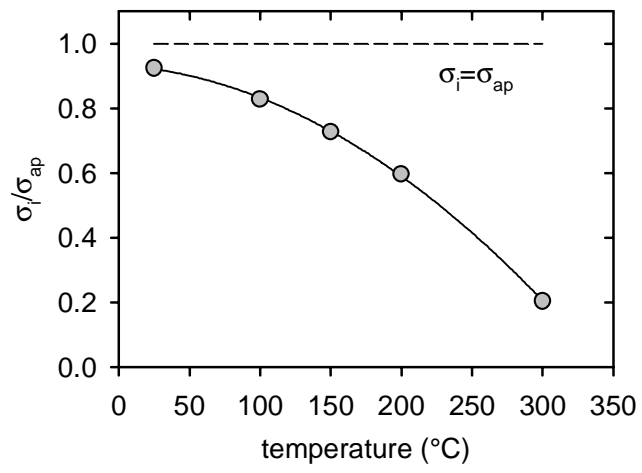


Fig. 7